10

Moons, asteroids, and comets interacting with their surroundings

MARGARET G. KIVELSON

A body such as a planet, a moon, an asteroid, or a comet, typically enveloped in a tenuous neutral gas, perturbs its surroundings in a flowing, magnetized plasma. The structure of field and plasma resulting from the interaction depends on properties of the plasma and of the body onto which the plasma flows. This chapter addresses the interaction of solar-system plasmas with a number of small bodies of the solar system. Size is taken as criterion, but we do not include small planets even though the biggest moons are similar in size to the smallest planet, Mercury. For reviews of planetary magnetospheres, see Chs. 10 and 13 in Vol. I.

Given that the Moon has no atmosphere, one might suppose that our discussion focuses on bodies that lack atmospheres, but that is not the case. Some moons, including small ones, are enveloped in neutral clouds that are not gravitationally bound but are, in many ways, similar to atmospheres. Other important properties differ from one body to another. Some moons have icy outer layers while others have outer layers of silicates and other non-icy materials; some have conducting regions in their interiors whereas others do not; and some are magnetized but others are not. Like the planets, the bodies that we discuss are spread throughout the solar system. Correspondingly, the plasma conditions vary from one to another. The focus on moons and comets is arbitrary, but the examples that we shall discuss are diverse and illustrate a large range of physical processes that can occur in the solar system. The interaction regions surrounding the small bodies of interest vary in global geometric configuration, in spatial extent relative to the size of the central body, and in the nature of the plasma disturbances. The objective of the discussion is to understand the physical processes that account for the observed features of the interaction regions.

10.1 Physics of large-scale processes in space plasmas

It is useful to start by discussing the physical principles that govern the behavior of the flowing, magnetized plasmas in which moons and comets are embedded.

The plasma of the space environment is a partially ionized gas, usually dominated by the ionized component. The physical principles that govern the behavior of the flowing medium differ from those that describe a neutral gas. In a neutral gas, collisions among the constituent atoms and/or molecules play a major role in the dynamics. In a magnetized space plasma, collisions are generally very infrequent and electromagnetic interactions control the behavior of the system. Symmetry is broken from the start by the presence of a magnetic field. Strong Coulomb forces maintain net charge neutrality within spatial volumes large enough to contain many ions and electrons, but ion and electron motions may differ enough to generate electric current. In the presence of a magnetic field, currents exert forces, adding to the complexity of the physical environment.

On large spatial and temporal scales, the properties of a magnetized plasma are governed by a combination of fluid equations and Maxwell's equations of electromagnetism, i.e., the equations of magnetohydrodynamics (MHD). Here, we examine the basic equations, not with the intention of mathematical manipulation, but with a desire to make clear how forces and responses are linked. The MHD equations are provided in Ch. 3 of Vol. I (see Table 1.2 for a chapter listing in all volumes), but here we are interested in somewhat different conditions. We neglect gravitational forces but include the sources and losses linked to ionization of neutrals, charge exchange, and associated processes. The equations that express the conservation of mass and momentum can be written as

$$\frac{\partial \rho}{\partial t} + \nabla \cdot \rho \mathbf{u} = S - L \qquad \text{(mass)} \tag{10.1}$$

$$\begin{aligned}\left(\frac{\partial \rho \mathbf{u}}{\partial t} + \nabla \cdot \rho \mathbf{u}\mathbf{u}\right) &= \rho\left(\frac{\partial \mathbf{u}}{\partial t} + \mathbf{u} \cdot \nabla \mathbf{u}\right) + \mathbf{u}(S - L) \\ &= \nabla p + \mathbf{j} \times \mathbf{B} + (\mathbf{S}_p - \mathbf{L}_p) \quad \text{(momentum)}\end{aligned} \tag{10.2}$$

where the first equality in Eq. (10.2) makes use of Eq. (10.1). To these equations, we add two of Maxwell's equations,

$$\frac{\partial \mathbf{B}}{\partial t} = -\nabla \times \mathbf{E} \qquad \text{(Faraday's law)} \tag{10.3}$$

$$\nabla \times \mathbf{B} = \mu_0 \mathbf{j} \qquad \text{(Ampere's law).} \tag{10.4}$$

In Eq. (10.4), we have assumed that the processes of interest occur on time scales that are sufficiently long to justify omission of the displacement current. In this, as yet incomplete, set of equations, ρ is mass density, $\mathbf{u}$ is bulk flow velocity, S and L are the source and loss rates of ion mass per unit volume, respectively, p is thermal pressure, $\mathbf{j}$ is current density, $\mathbf{B}$ is magnetic field, $\mathbf{S}_p$ and $\mathbf{L}_p$ are source and

loss rates of momentum density per unit volume, $\mathbf{E}$ is the electric field, and μ_0 is the permeability of vacuum. Sources and losses are of exceptional importance for comets, which emit gases and dust when their surfaces heat up as they approach the sun. Some moons have atmospheres or geysers, and for them, too, sources and losses may be extremely important.

One can write Eq. (10.2) that governs the momentum density in the following useful form

$$\frac{\partial \rho \mathbf{u}}{\partial t} = -\nabla \left(p + \frac{B^2}{2\mu_0} + \rho u^2 \right) + \mathbf{B} \cdot \nabla \mathbf{B}/\mu_0 + (\mathbf{S}_p - \mathbf{L}_p). \tag{10.5}$$

Here, the quantities $B^2/2\mu_0$ and ρu^2 enter as additions to thermal pressure. These terms are referred to as the magnetic pressure and the dynamic pressure, respectively. The term $\mathbf{B} \cdot \nabla \mathbf{B}/\mu_0$ is referred to as the curvature force (actually force density) and acts like tension in a string to accelerate plasma towards the center of field line curvature.

The electric field can be related to $\mathbf{u}$ and $\mathbf{j}$ through a form of Ohm's law: $\mathbf{E} = -\mathbf{u} \times \mathbf{B} + \eta \mathbf{j}$, where η is the resistivity. When the resistivity becomes sufficiently small, as is the case in most parts of the systems that we consider, the last term in this equation can be omitted and the electric field is given by

$$\mathbf{E} = -\mathbf{u} \times \mathbf{B}. \tag{10.6}$$

Equation (10.6) can be used to rewrite Eq. (10.3) as

$$\frac{\partial \mathbf{B}}{\partial t} = \nabla \times (\mathbf{u} \times \mathbf{B}). \tag{10.7}$$

The resulting system of equations is referred to as ideal MHD, which is a description that we will find particularly useful.

Equations (10.1), (10.2), (10.4), and (10.7) are still incomplete as one can confirm by counting the number of unknowns (11) and the number of equations (10), recognizing that a vector or a vector equation has three components. In Ch. 3 of Vol. I, an approximation to energy conservation (their Eq. (3.3)) was used to complete the set of equations, but here we complete the description using the adiabatic assumption that relates pressure to density:

$$p\rho^{-5/3} = \text{constant} \quad \text{(adiabatic condition)}. \tag{10.8}$$

Now we have 11 equations in 11 unknowns.

One may wonder why we have omitted two of Maxwell's equations, i.e., Poisson's equation that relates $\mathbf{E}$ to the charge density and the requirement that $\mathbf{B}$ be divergence free ($\nabla \cdot \mathbf{B} = 0$). Actually the latter can be incorporated in our analysis as an initial condition. The divergence of Eqs. (10.3) or (10.7) requires that

$\partial(\nabla \cdot \mathbf{B})/\partial t = 0$ so if the divergence of $\mathbf{B}$ is set to zero at any time, it will remain zero at all times. Poisson's equation is not used because we require the charge density, and correspondingly $\nabla \cdot \mathbf{E}$, to be negligibly small, i.e. of order the terms we have dropped in the approximations used to write the equations that we retain.

From the ideal MHD equations it becomes evident that currents affect flows (Eq. (10.2)), but also that flows change the magnetic field (Eq. (10.7)) and changes of the magnetic field modify the current (Eq. (10.4)). The complex coupling leads to interesting physics. When a plasma flows onto a solid body, or even a dense atmosphere, it is usually slowed and diverted, just as the flow of a stream of water is slowed and diverted by an obstacle in its path. As the flow changes, the local structure of the magnetic field changes and generates current that modifies the flow. In space, multiple properties are inextricably linked.

Although the equations provided in this section treat plasmas as fluids, some concepts are better presented in terms of the behavior of ions and electrons. For example, the Lorentz force law, $\mathbf{F} = q(\mathbf{v} \times \mathbf{B})$, with $\mathbf{F}$ the force on a particle of charge q moving at instantaneous velocity $\mathbf{v}$ in a magnetic field, tells us that magnetic forces do not change the component of velocity along a field but impose force across the field. (Note the distinction between the velocity of an individual charged particle, $\mathbf{v}$, and the bulk flow velocity, $\mathbf{u}$, which is the mean velocity of a collection of particles.) Charged particles move in helical paths along the field, right-handed for electrons and left-handed for ions. The effect is to tie the plasma to the magnetic field. The tight link between a flux tube and its plasma content is described as the frozen-in field condition and is discussed at length in Ch. 4 of Vol. I. The theorem, valid for ideal MHD, states that if two fluid elements lie on a common field line at one time, then they lie on a common field line at all times. The concept can be exploited to account for changes of the flux tube structure imposed by the properties of the plasma flow. More important, the theorem makes clear that interpenetration of distinct magnetized plasmas requires a breakdown of ideal MHD.

10.2 Characterizing the plasma that interacts with solar-system bodies

As obstacles to the flow, moons and comets create local disturbances in the plasmas in which they are embedded. The specific structure that envelopes the body depends on properties of the ambient plasma and these properties vary greatly depending on whether the external plasma is the rapidly flowing and temporally variable solar wind or the slowly flowing plasma of a planetary magnetosphere. The typical plasma density, temperature, and magnetic field intensity also vary from one case to another. Consequently, it may seem unlikely that general rules can describe the interaction regions.

We are rescued from the need to treat each case as totally distinct by recognizing that physical theories often incorporate a small set of dimensionless parameters that control important aspects of a system, even if such properties as spatial scale, temperature, and flow velocity vary by many orders of magnitude. For a flowing plasma incident on an obstacle, the form of the interaction depends critically on how the flow speed is related to the speed of waves that transmit information about changes of plasma properties from one part of the system to another. An analogy to waves in neutral gases helps to clarify the concept. In the frame of an airplane in flight, the atmosphere flows onto the plane at some velocity, call it $\mathbf{u}$. As the gas encounters the plane, pressure perturbations develop. Pressure perturbations launch sound waves that travel at the sound speed, c_s. If such waves can move away from the plane, they can divert the atmosphere upstream of the plane. But the waves are swept back toward the plane at the flow speed of the plasma. Only if $u < c_s$ is it possible for the waves to begin to divert the atmosphere well upstream of the plane. If $u > c_s$, as for a supersonic jet, the waves pile up in front of the plane, causing a shock to develop upstream. Only downstream of the shock is the flow diverted. Assuming that the plane is large compared with distances characteristic of atmospheric properties, the parameter that determines whether or not a shock will form is the (dimensionless) sonic Mach number of the surrounding atmosphere, u/c_s.

In a plasma, much as in a neutral gas, compressional perturbations develop when there is an obstacle in the flow. The sound speed is relevant to understanding how such perturbations propagate through the system, but in a plasma, there are waves that differ from sound waves and change both the field and the plasma. Because the form of the disturbances in the vicinity of a moon or other small body depends so strongly on the nature of the waves that carry perturbations through the plasma, we digress to describe the properties of some characteristic wave modes.

10.2.1 Magnetohydrodynamic waves

The waves that carry information through a magnetized plasma differ from the sound waves of a neutral gas, partly because of the anisotropy imposed on the fluid by a magnetic field and partly because the waves must be capable of carrying currents that modify the properties of both matter and magnetic field. The properties of such waves can be derived from the MHD Eqs. (10.1)–(10.8) by analyzing the evolution of small perturbations.

Consider a uniform plasma with constant pressure and density (p and ρ) whose center of mass is at rest ($\mathbf{u} = 0$). Assume that a constant background field ($\mathbf{B}$) is present and that neither sources nor losses need be considered. Small departures from this background state are taken to vary with space ($\mathbf{x}$) and time (t) as $e^{i(\mathbf{k}\cdot\mathbf{x}-\omega t)}$. Here, $\mathbf{k}$ is the wave vector and ω is the angular frequency of the wave. Perturbations

occur in density $d\rho$, velocity $\mathbf{du}$, pressure dp, current $\mathbf{j}$, and field $\mathbf{b}$. Terms linear in small quantities in Eqs. (10.1) and (10.5) satisfy

$$-\omega d\rho + \rho \mathbf{k} \cdot d\mathbf{u} = 0 \tag{10.9}$$

$$-\omega\rho d\mathbf{u} = -\mathbf{k}dp + \mathbf{b}(\mathbf{k} \cdot \mathbf{B})/\mu_0 - \mathbf{k}(\mathbf{b} \cdot \mathbf{B})/\mu_0. \tag{10.10}$$

Equation (10.8) gives the pressure perturbation in terms of the density perturbation as

$$dp/p = \gamma d\rho/\rho \tag{10.11}$$

and Eq. (10.7) implies

$$\omega\mathbf{b} = d\mathbf{u}(\mathbf{k} \cdot \mathbf{B}) - \mathbf{B}(\mathbf{k} \cdot d\mathbf{u}). \tag{10.12}$$

The solutions to Eqs. (10.9) to (10.12) are the roots of the equation

$$(\omega^2 - v_A^2 k^2 cos^2\theta)[\omega^4 - \omega^2 k^2 (c_s^2 + v_A^2) + k^4 v_A^2 c_s^2 cos^2\theta] = 0, \tag{10.13}$$

where θ is the angle between $\mathbf{k}$ and $\mathbf{B}$, and the Alfvén speed (v_A) and the sound speed (c_s) have been introduced. These quantities characterize the speed of propagation of waves in a magnetized plasma and are defined by

$$v_A^2 = B^2/2\mu_0\rho \tag{10.14}$$

$$c_s^2 = \gamma p/\rho. \tag{10.15}$$

The sound speed has the form familiar for a neutral gas. The Alfvén speed is a second natural wave speed characteristic of a magnetized plasma. Just as we introduced the (dimensionless) sonic Mach number as the ratio of the flow speed to the sound speed, it is useful to define a dimensionless Mach number, the Alfvénic Mach number ($M_A = u/v_A$), related to the Alfvén speed.

As mentioned previously, the quantity $B^2/2\mu_0$ is the pressure exerted by the magnetic field, so both of the basic wave speeds are proportional to the square root of a pressure divided by a density. The ratio of the thermal pressure to the magnetic pressure is another useful dimensionless quantity, for which we use the symbol, β, defined as $\beta = p/(B^2/2\mu_0)$. When $\beta < 1$, magnetic effects dominate the effects of the thermal plasma, but in a high-β plasma, the plasma effects dominate.

Equation (10.13) is of sixth order in ω/k with three pairs of roots. One pair results from setting the first factor in Eq. (10.13) to zero; the resulting dispersion relation is

$$(\omega^2 - v_A^2 k^2 cos^2\theta) = 0. \tag{10.16}$$

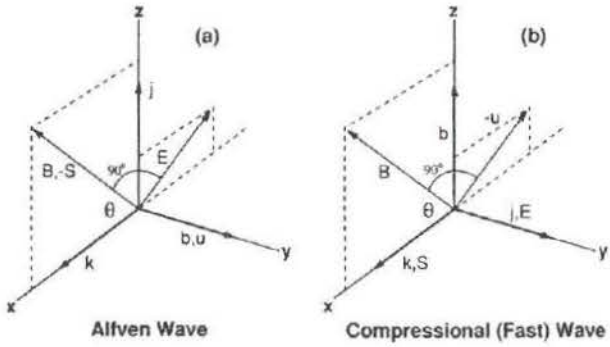

Fig. 10.1 Polarization of MHD waves in a uniform medium. The parameters other than **S** are defined in the text and are plotted with the wave vector along the x-axis and the background field (**B**) in the $x-z$ plane. The incompressible Alfvén wave polarization is plotted on the left and the compressional fast wave polarization is plotted on the right. **S** is the Poynting vector oriented in the direction in which energy density is transported by the wave: strictly field-aligned for the Alfvén wave and oblique for the compressional wave. (From Kivelson, 1995.)

This solution describes waves referred to as Alfvén waves. For this dispersion relation to apply, the magnetic perturbation must be perpendicular to both **B** and **k** (see Fig. 10.1). This orientation implies that to first order in small quantities, the Alfvén wave does not change the field magnitude $[(\mathbf{B}+\mathbf{b})^2 = B^2 + 2(\mathbf{B}\cdot\mathbf{b})^2 + b^2 \approx B^2]$. The wave phase speed is $v_{ph} = \omega/k$ and $v_{ph} = \pm v_A cos\theta$. Waves carry information at the group velocity, $\mathbf{v}_g = \nabla_k \omega$, where the subscript on the gradient indicates that the derivatives are taken in **k** space; the solution is $v_g = \pm\hat{\mathbf{B}}v_A$ where $\hat{\mathbf{B}}$ is a unit vector along the background field. The remarkable property of these waves is that they carry information only along the background field, and they bend the field without changing its magnitude. These properties are of considerable importance in interpreting the interaction of a flowing plasma with the solid bodies of the solar system.

Equation (10.13) has two more pairs of roots, the zeros of the fourth order polynomial in square brackets in Eq. (10.13), i.e., the solutions

$$v_{ph}^2 = \omega^2/k^2 = \frac{1}{2}\left(c_s^2 + v_A^2 \pm [(c_s^2 + v_A^2)^2 - 4v_A^2 c_s^2 cos^2\theta]^{1/2}\right). \qquad (10.17)$$

The solutions (two pairs, one positive and one negative, of roots) correspond to what are unimaginatively referred to as fast (or magnetosonic) and slow mode waves. The wave perturbations of both modes may have magnetic perturbations along and across **B** (see Fig. 10.1b). Perturbations along **B** change the field magnitude and the thermal pressure. The fast-mode changes of thermal and magnetic pressure are in phase with each other; this implies that the total pressure fluctuates.

The slow-mode changes of thermal and magnetic pressure are in antiphase, and the total pressure fluctuations are very small. For waves propagating along the background field ($cos\theta = \pm 1$), the solutions to Eq. (10.17) are c_s^2 and v_A^2, with the larger of the two applying to the fast mode. For waves propagating at right angles to the background field ($cos\theta = 0$), the wave speeds are $c_s^2 + v_A^2$ and 0, indicating that only fast mode waves propagate across the field.

10.2.2 Selected properties of the upstream flow

Having identified some of the waves that carry information through a magnetized plasma, we are now able to introduce the dimensionless parameters that help us understand aspects of flow and field perturbations. The magnetosonic Mach number (M_{ms}) is the ratio of the flow speed to the fast-mode speed, taken as $(c_s^2+v_A^2)^{1/2}$. M_{ms} reveals whether or not a shock is likely to form upstream in the flow. When $M_{ms} < 1$, compressional waves can travel upstream from the obstacle faster than the flowing plasma can sweep them back. These waves, moving upstream, can divert the incident flow around the obstacle, much as the bow wave of a ship diverts water to the sides, and no shock develops. However, as in the situation discussed in the context of supersonic flight, if $M_{ms} > 1$, compressional waves are unable to propagate upstream faster than they are swept back by the flow. They pile up to form a shock. Most bodies in the super-magnetosonic solar wind (exceptions are discussed in Sect. 10.8) create shocks standing somewhat upstream on their sunward sides. Downstream of the shock, plasma is heated, compressed, and diverted around the obstacle.

The Alfvén Mach number (M_A) is the ratio of the speed with which the ambient plasma flows towards an obstacle divided by the Alfvén speed. We will see that this quantity controls the shape of the interaction region in planes containing the unperturbed plasma flow and the background magnetic field. The plasma beta (β) is the ratio of the thermal pressure to the magnetic pressure. This quantity enables us to understand how significantly the magnetic field structure can be modified by changes of the plasma pressure.

The plasma environment differs greatly among the small bodies of the solar system. Some of the bodies are embedded in the solar wind, others in the plasma of a planetary magnetosphere, and some (such as Earth's Moon) move from one environment to another.[1] Table 10.1 lists some plasma properties relevant to the environment of selected bodies. In Sect. 10.4, we discuss further how M_A and β control aspects of the interaction. However, we shall first consider how various properties of the obstacle affect the interaction.

[1] The Moon orbits the Earth at a distance of 60 Earth radii. It spends part of each lunar month in Earth's magnetotail and the rest of the month in the solar wind.

Table 10.1 *Properties of the plasmas upstream of selected small bodies of the solar system.*

Obstacle	Ambient plasma	M_A	M_{ms}	β
Io, Europa, Ganymede	Jovian magnetosph.	< 1	< 1	< 3
Asteroids	Solar wind	> 1	> 1	~ 1
Comets	Solar wind	> 1	> 1	~ 1
Moon	Earth's magnetosphere or solar wind	either > 1 or < 1	either > 1 or < 1	~ 1 or < 1

10.3 Effects of the electrical properties of an obstacle in the flow

Currents flow readily in an ionized gas. If the plasma flows onto a solid body, one anticipates that the electrical properties of the obstacle will affect the interaction, and they do. Bodies like the Moon have no atmosphere and are very poor conductors but many solid bodies of the solar system are surrounded by an ionized region or a cloud of neutrals that can be ionized and can conduct electricity. Currents can also flow in plasmas trapped in the magnetic field of a magnetized body. The presence or absence of a conducting path through a body or its surroundings greatly affects the form of interaction with a flowing plasma.

10.3.1 Flow patterns at non-conducting or conducting bodies

A plasma flowing at velocity $\mathbf{u}$ generates an electric field, the $-\mathbf{u} \times \mathbf{B}$ electric field of Eq. (10.6). Correspondingly, in the unperturbed flow, an electric potential drop is present across distances separated perpendicular to the background field, such as the distance marked $2R_M$ in Fig. 10.2a. The form of the interaction of the plasma with a body immersed in the flow is significantly affected by the electrical conductivity of the body through responses that we consider here.

Earth's Moon is an excellent example of a very poor conductor. A poor conductor (like a capacitor) can develop surface charge consistent with the electric field across it. Despite the development of surface charge, no current will flow because of the low conductivity. The electric potential of the surface charges will cancel the potential drop in the solar wind. In this situation, no force is imposed on the plasma, which flows without obstruction onto the surface (see Fig. 10.2a). The magnetic field of the incident plasma penetrates the body and is present throughout the interaction region. The principal effect of the interaction is to deplete plasma in the region downstream in the wake. In this region the magnetic pressure increases to produce pressure balance with the plasma surrounding the wake. Below we discuss how the wake refills.

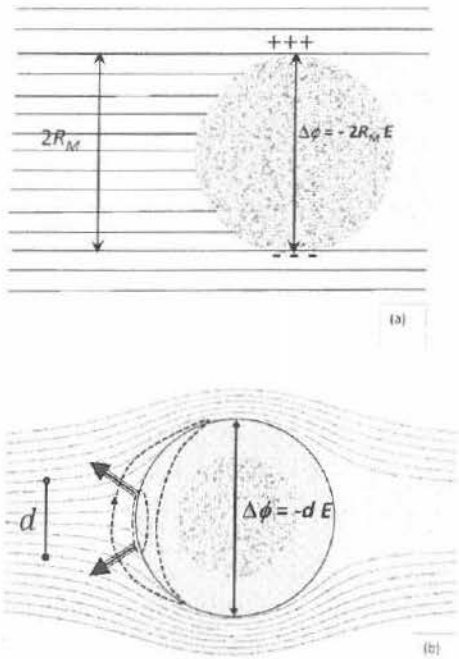

Fig. 10.2 Schematics of plasma flow (shown by lines of flow) at velocity $\mathbf{u}$ from the left onto (a) a non-conducting body and (b) a conducting body. In the plasma, $\mathbf{B}$ is into the paper, $\mathbf{E}$ is $-\mathbf{u} \times \mathbf{B}$ in both cases. Diagram (a) shows that a non-conducting body builds up surface charge that imposes a potential drop $\Delta\phi = -2R_M E$ across the diameter, producing an electric field that opposes the solar wind electric field. Diagram (b) shows the response of a conducting body that does not build up surface charge. Conducting paths allow current (shown schematically as a dashed line) to flow through the body and close in the incident flow. Heavy-banded arrows identify the orientation of the resultant $\mathbf{j} \times \mathbf{B}$ force that diverts part of the incident flow. Because much of the incident flow has been diverted, the potential drop across the body is only $\Delta\phi = dE$, where $d < R_M$ is the distance in the incident flow between the flow lines that just graze the body. The electric field that penetrates the body is a fraction of the upstream field determined by the fraction of the upstream flow that impacts the surface. In the wake region, gray in both diagrams, the plasma pressure is reduced and the magnetic pressure is increased relative to the upstream values.

If the body can conduct current, the response is quite different. For a sub-magnetosonic upstream flow, there is no bow shock. The schematic of Fig. 10.2b shows the plasma incident on a body with a conducting outer shell. In the absence of a local response, the upstream plasma within a cylinder of radius R_M about a line through the center would flow onto the moon's surface. However, in response to the electric field of the flowing plasma, current begins to flow either through a solid outer layer or through the ionized gas layers that envelope many solar-system

bodies. Where the current emerges from the conducting layer, it comes in contact with the incident plasma and closes through it. In equilibrium, the current flowing through the plasma exerts a $\mathbf{j} \times \mathbf{B}$ force (see Eq. (10.2)) that diverts some of the incident flow as illustrated in Fig. 10.2b. Only a portion of the plasma that flows through the cylindrical volume that maps from upstream along unperturbed flow lines to the moon's cross section actually contacts the surface because some plasma is diverted around the sides. The maximum potential drop across the body then corresponds to the potential drop across the portion of the unperturbed flow (marked d in the figure) that actually reaches the surface; this potential drop is smaller than for a non-conducting body. In this case, the interaction modifies the flow well upstream of the moon, and the wake that develops is narrower than in the non-conducting case. If the conductivity of the body is extremely high, almost all of the plasma is diverted to the side, implying that d approaches 0 and correspondingly there is no potential drop across the body.

10.3.2 Pickup ions, neutrals, and associated currents

At comets and in the vicinity of moons, such as Io and Enceladus, that are significant sources of neutral gas, various processes that convert neutral atoms or molecules into ions are important to consider. Neutrals can be ionized by photons (photoionization) or by collisions with other particles, typically electrons (impact ionization). An additional process that affects the interaction region is charge exchange. In this process, a neutral gives up a charge to an ion. The original ion, now neutral, carries off its incident momentum while the original neutral becomes an ion at rest in the frame of the neutral gas.

The ions introduced into the plasma by ionization of neutrals modify the bulk properties of the plasma. Consider a situation in which the neutrals are at rest relative to the obstacle, towards which the plasma flows at (bulk) velocity $\mathbf{u}$. Photoionization and impact ionization add mass to the plasma whereas charge exchange between the ionized or neutral form of the same element does not change the mass density. All three processes slow the bulk flow because the new ions must be accelerated so that their average motion matches that of the bulk plasma and the process extracts momentum from the incident plasma. These processes also change the thermal energy of the plasma (e.g., Linker *et al.*, 1998) and may modify the plasma composition. The complex effects associated with pickup can significantly modify the interaction region surrounding a moon or a comet.

The relation between pickup and currents is shown schematically in the left-hand part of Fig. 10.3. The newly ionized ion senses the electric field of the flowing plasma and begins to move in the direction of this electric field. The electron that has separated from the ion is initially accelerated in the opposite direction. After

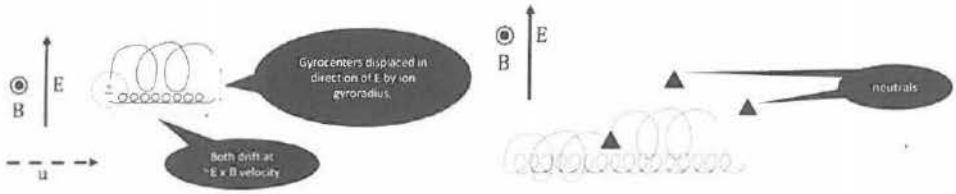

Fig. 10.3 Schematic of interactions with plasma with neutrals. Left: initial motion of pickup ions and electrons. The gray circle represents a neutral composed of a positively charged ion and a negatively charged electron. The directions of plasma flow velocity, **u**, of the magnetic field, **B**, and of the electric field, **E**, are indicated. In the image, following dissociation, the ion path starts upward and the electron path starts downward. Although initial motion is along **E** for the ion, the Lorentz force causes the path to twist, resulting in motion around **B** at the ion cyclotron period, leading to a net drift at a velocity of $\mathbf{E} \times \mathbf{B}/B^2$. The electron initially moves in the $-\mathbf{E}$ direction. Its motion also rotates around B, but at the electron cyclotron frequency. The net effect is a transient current in the direction of **E**. Right: schematic of the effect of collisions with neutrals for a case with the collision frequency of order the ion cyclotron frequency. The triangles represent neutrals. The effect of collisions is to slow the motion in the $\mathbf{E} \times \mathbf{B}$ direction of the ions but not of the electrons and to displace the ions in the direction of **E**. A net current arises, with one component along $-\mathbf{E} \times \mathbf{B}$ (a Hall current) and one component along **E**, a Pedersen current.

one gyroperiod, the average separation of the gyrocenters of the two charges is close to one ion gyroradius

$$\rho_g = m_{ion} v_{ion}/qB, \tag{10.18}$$

where m_{ion} is the ion mass, v_{ion} is its thermal velocity, and q is its charge. The result of the separation of charges is to produce a transient current density in the direction of the electric field. If the pickup is occurring at a rate $\dot{n}$, where $\dot{n}$ is the number of ionizations per unit volume and time, then the pickup current is

$$j_{pickup} = q\dot{n}\rho_g. \tag{10.19}$$

Because pickup current flows across the background field, a cloud of pickup ions acts much like a solid conducting obstacle in the flow and imposes the same types of perturbations, i.e., it slows and diverts the incident flow and produces bendback of the field in Alfvén wings in the manner described in Sect. 10.4.

Neutral gas density is often enhanced around a moon because material is continually sputtered off the surface, or because there are geysers (Enceladus) or volcanoes (Io), or because it has enough gravity to retain an atmosphere (Titan). In that case, current can arise in the plasma through collisions in a manner illustrated schematically on the left side of the right-hand diagram in Fig. 10.3. Current

driven along **E** is referred to as Pedersen current. Current driven in the $-\mathbf{E} \times \mathbf{B}$ direction and carried by electrons is Hall current.

10.4 The interaction region and the role of MHD waves

In the discussion of Sect. 10.3.1, the slowing and diversion of the upstream flow was described in terms of currents, but it is more instructive to think of changes in the incident plasma being imposed by waves. Section 10.2 introduced the properties of the MHD waves that carry perturbations through a magnetized plasma. The fastest waves propagate farthest upstream in the flow. In this discussion, we assume that there are conducting paths either through the moon or other body or in its surroundings. Figure 10.1b shows that fast magnetosonic waves carry current density, **j**, perpendicular to the background field. The fast waves set up pressure gradients in the flow upstream of the obstacle, and Eq. (10.5) shows that, in the absence of sources and losses, a gradient of total pressure (the sum of thermal and magnetic pressure) can decelerate the flow. (The curvature term is insignificant in most of the situations that we consider.) Indeed, fast magnetosonic waves propagating upstream slow and divert the plasma upstream of a conducting obstacle. Because these waves can propagate along or across the field, the process is not greatly affected by the field orientation. As mentioned previously, if the upstream flow is super-magnetosonic, a shock forms upstream of a conducting body, and the shock, a steepened fast magnetosonic wave, imposes the slowing and the diversion of flow.

Once the flow has been modified by the effects of the fast mode waves, perturbations linked to the other two wave modes affect the interaction. Again, we start by describing the interaction in a sub-magnetosonic flow. Figure 10.4 presents two views of the interaction region, in (a) a cut through the center of the body in the plane containing the upstream flow and the unperturbed magnetic field ($x-z$ plane) and in (b) a cut through the center of the body and transverse to the upstream flow ($y-z$ plane). (Figure 10.2b completes the schematic illustration in a plane perpendicular to the two illustrated in Fig. 10.4.) In Fig. 10.4a, the slight bends of the field just upstream of the moon illustrate the compression imposed by the fast mode wave. This compression diverts the flow away from the central bulge in a direction perpendicular to the background field and the flow. Equation (10.12) shows that the flow diversion implies a magnetic perturbation transverse to the plane of the illustration in Fig. 10.4a. The perturbations propagate up and down along the background field as Alfvén waves. However, the propagation of these waves along the background field must be viewed in the rest frame of the plasma. (Recall that, in deriving the properties of Alfvén waves, we set the background flow velocity to 0, thus implying that the analysis was carried out in the plasma rest frame, where we

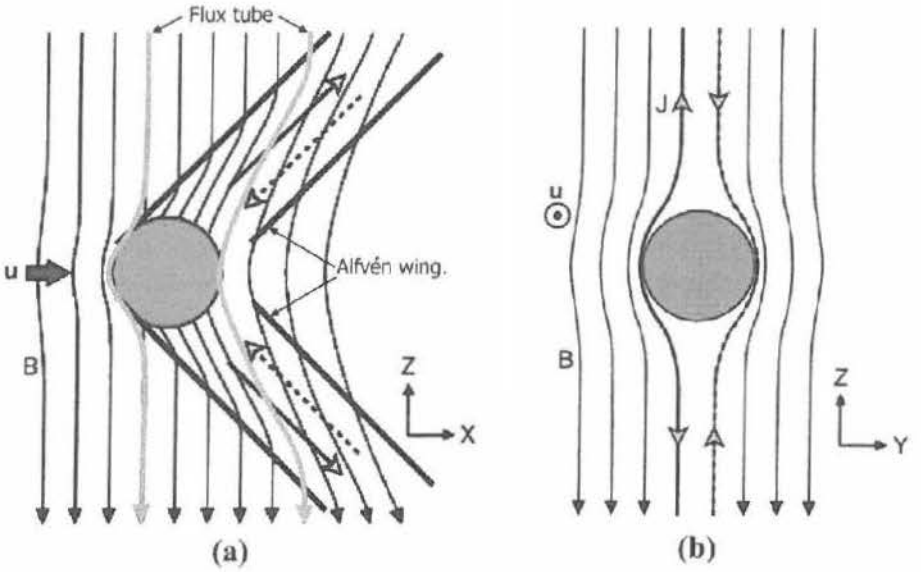

Fig. 10.4 Schematic representations of the interaction of a conducting body in a sub-magnetosonic plasma flow. (a) A cut through the center of the moon in the plane of the unperturbed field and the incident flow; (b) a cut through the center of the moon in the plane perpendicular to the incident flow. Field lines are thin black lines with black arrowheads but are shown in gray on the edges of the flux tube containing field lines that penetrate the obstacle, the Alfvén wing boundaries are thick black lines, the upstream flow is shown as a heavy black arrow labeled **u**, currents are black lines with open arrowheads, solid where the currents are directed away from the moon and dashed where they are directed towards the moon. (From Jia *et al.*, 2010.)

found that these waves carry information only in the direction $\pm\mathbf{B}$.) In Fig. 10.4, the plasma is moving at velocity **u** with respect to the body, taken to be at rest. Because the signal moves along the field in the moving rest frame, the signal can be present only downstream of the left-hand pair of heavy black lines in Fig. 10.4a. The region in which the strong field perturbations develop is called an Alfvén wing.

Figure 10.4a shows projections of bent field lines, although the actual bends are out of the plane of the image. The Alfvén wave does not change the field magnitude which is approximately constant across the boundaries in the illustration. Field-aligned currents flow on the boundaries of the region where Alfvénic perturbations are important and become weak in the region downstream of the right-hand pair of heavy lines on the right in Fig. 10.4a. Arrows in the figure indicate the direction in which current flows near the boundaries behind (dashed arrow) and in front (solid arrow) of the plane of the image. These currents are also shown in the plane perpendicular to the upstream flow in Fig. 10.4b. Downstream of the Alfvén wing,

the slow mode begins to play a role in a region where the plasma pressure increases while the magnetic pressure decreases.

The situation illustrated in Fig. 10.4 represents interaction for M_A slightly less than 1. Near 1 AU (the radius of Earth's orbit around the Sun) in the solar wind, M_{ms} is typically of order 6. After passing through the bow shock, the flow speed diminishes, but still remains substantially larger than v_A. This means that downstream of Earth's bow shock the field must bend through an angle far greater than that shown in the figure. That is why Earth's magnetospheric boundary bends back so far that it forms the bullet-shaped cavity with which we are familiar.

The attentive reader will have noticed that Fig. 10.4 shows currents converging on the moon on one side and diverging from the moon on the opposite side. Currents are divergenceless, so there must be closure paths across the magnetic field direction that link the converging currents on the right of Fig. 10.4b to the diverging currents on the left, i.e., current must flow across the magnetic field in the near vicinity of the moon. If the moon itself is a good conductor, the current can close through it. Otherwise, it must close through the plasma in its immediate surroundings. The mechanisms that enable such closure currents to flow were discussed in Sect. 10.3.2.

10.5 Moons with magnetic fields permanent or inductive

We have discussed the interaction with small bodies assuming that the body is not magnetized and the plasma magnetic field is constant in time. Of course, these assumptions may not be valid. In particular, Jupiter's moon Ganymede, has a permanent internal magnetic moment and, for some moons, the periodic variation of the external magnetic field may drive an inductive response, thereby generating a varying internal magnetic field. Here, we consider these situations.

10.5.1 Ganymede, a magnetized obstacle

Prior to the Galileo Orbiter's first close pass by Ganymede, it seemed unlikely that so small a body (radius 2634 km) would have a magnetic field. Skepticism was justified because a planetary dynamo (see Ch. 6) requires an internal region of molten metal and it was thought that small bodies in the outer solar system would have cooled to a temperature at which even the deep interior would be solid. Thus it was a surprise when Galileo measurements revealed that Ganymede has a rather large dipole moment oriented nearly parallel to Jupiter's equatorial field, with equatorial surface intensity of $B_{eq} = 720\,\text{nT}$. Ganymede is embedded in Jupiter's magnetospheric plasma, which flows towards the moon at a speed of approximately 140 km/s. Because to a good approximation, Jupiter's magnetospheric field

is frozen into the flowing plasma (see Sect. 10.1), it cannot penetrate into the region dominated by Ganymede's internal field, but instead flows around it. In this situation, the interaction region is justifiably referred to as a magnetosphere. By definition, Ganymede's magnetosphere is the region embedded within Jupiter's magnetosphere that is threaded by the field lines with at least one end at the moon. The magnetosphere is unique. It is the only one that lies within a planetary magnetosphere because no other moon is known to possess a permanent internal magnetic moment. The size of Ganymede's magnetosphere is established by pressure balance, with the external pressure being $p + B^2/2\mu_0 + \rho u^2$ (see Eq. (10.5)) and the internal pressure well approximated as the magnetic pressure at distance r from its center of a dipole field centered within Ganymede. In Jupiter's magnetosphere near the orbit of Ganymede, the magnetic field magnitude is roughly 100 nT and magnetic pressure (4 nPa) dominates the contributions of thermal and dynamic pressure. Along the meridian containing the upstream flow, $\mathbf{u}$, pressure balance requires $[B_{eq}/(r/R_G)^3]^2 2/2\mu_0 = 4\,\text{nPa}$ or $r \sim 2R_G$.

Figure 10.5 shows the form of Ganymede's magnetosphere extracted from an MHD simulation by Jia *et al.* (2008). Evident in Fig. 10.5b is the fact that the

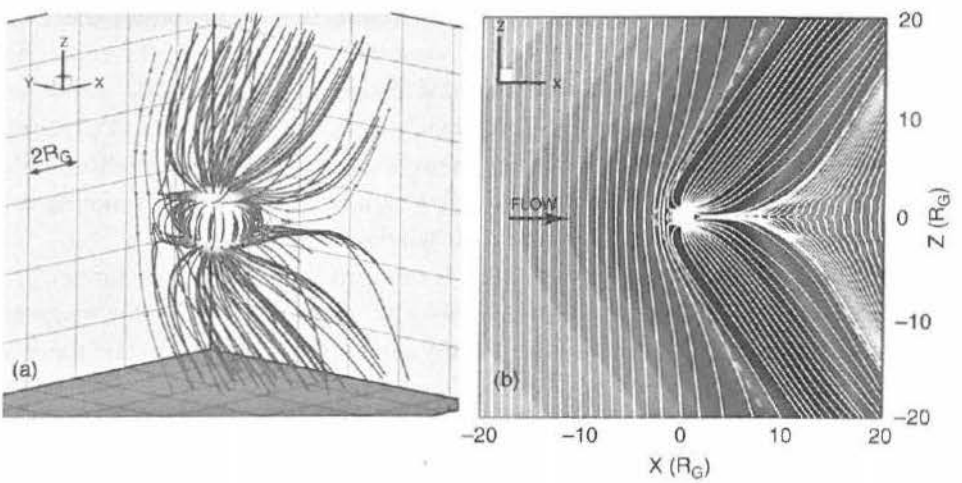

Fig. 10.5 (a) Selected magnetic field lines in Ganymede's magnetosphere from an MHD simulation. (b) Magnetic field lines projected onto the $x-z$ plane at $y = 0$. The x-component of the plasma flow velocity is shown in color. Orange dashed lines are tilted relative to the background field at the Alfvén angle and the flow is excluded from regions downstream of the left hand dashed lines, reappearing only in regions about 5 R_G further downstream. In the simulation, the sphere of radius 1.05 R_G is the inner boundary for plasma flow. (From Jia *et al.*, 2008.) A black and white version of this figure will appear in some formats. For the color version, please refer to the plate section.

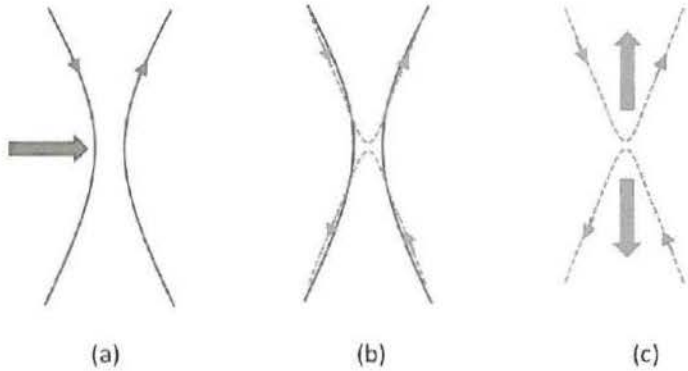

Fig. 10.6 Schematic of reconnection between oppositely oriented field lines. In (a) the southward-oriented field of Jupiter flows (heavy gray arrow) towards the northward-oriented field of Ganymede. In (b), the field lines reconnect so that the northern end of a Jovian field line continues into the northern end of a field line from Ganymede. In (c), the kinks in the newly connected field lines accelerate plasma to the north and the south, with gray arrows indicating the sense of flow.

upstream plasma does not flow into Ganymede's magnetosphere, but instead flows around it just as plasma would flow around a highly conducting body. A magnetic field acts as a barrier to plasma flow. The region in the equatorial plane from which the external plasma is excluded is substantially larger than the equatorial cross section of Ganymede, with the stand-off distance close to the $2R_G$ estimated. The shape of the magnetosphere differs greatly from the shape of Earth's magnetosphere because the symmetry of the system is dictated by the orientation of the external field, not by the direction of the plasma flow (see Table 10.1, noting that at Ganymede $M_A < 1$, whereas in the solar wind near Earth, $M_A > 1$).

At the orbit of Ganymede, Jupiter's field is oriented to the south, but Ganymede's equatorial field is oppositely oriented. This sets up the conditions for magnetic reconnection, a process in which oppositely directed field lines change the way they connect across a region in which their opposing orientation weakens the field. The process is shown schematically in Fig. 10.6. A fraction of the incident flow reconnects with the magnetic field of Ganymede, and produces the field lines seen in regions near the poles that are connected at one end to Ganymede and at the other end to Jupiter. (The field lines drawn to the upper and lower edges of the images in Fig. 10.5 should be regarded as continuing into Jupiter's ionosphere.)

Reconnection at Ganymede's magnetopause holds special interest for magnetospheric studies as an example in which the upstream plasma never rotates far from an orientation antiparallel to that of the internal field near the equator. This orientation implies that reconnection could occur in a relatively stable manner, as contrasted with the situation for planets in the solar wind exposed to fluctuating

orientations of the component of the field aligned with their internal magnetic moments. However, studies of reconnection at Ganymede suggest that even in the case of Jupiter's stable magnetosphere, reconnection is not steady but intermittent with a typical recurrence time of tens of seconds. The short time between bursts of reconnection has a parallel in Mercury's magnetosphere, where reconnection has been found to occur intermittently and also to recur in tens of seconds. At other planets, reconnection can be intermittent but with much longer characteristic repetition intervals ($\sim$8 min at Earth).

10.5.2 Europa and response to a varying external magnetic field

The reader may wonder why the discussion of Ganymede in the previous section included a statement, carefully framed, that refers to a permanent internal magnetic moment. The reason is that some moons that lack a permanent magnetic moment may have a varying magnetic moment if they are embedded in a varying magnetic field. Such a situation can arise if a moon has a global-scale conducting layer, possibly below its surface, and is embedded in a varying magnetic field.

A striking example is Europa. Magnetic perturbations observed on the first flyby of Europa by the Galileo Orbiter were well modeled as those imposed by an internal dipole moment pointing along the radial direction to Jupiter and perpendicular to Europa's spin axis. Like the other Galilean moons (Io, Ganymede, and Callisto), Europa's orbit lies in Jupiter's spin equator. Because Jupiter's dipole moment is tilted by 10° relative to its spin axis, the orientation of the field embedded in the plasma flowing around all of these moons varies at the synodic period of Jupiter's rotation, 11.23 h at Europa. The varying part of the external field is dominated by the component along a radius vector from Jupiter's center. Equation (10.3) implies that a varying magnetic field generates an inductive electric field. If all of Europa's interior or even a shell, consists of conducting matter, the inductive electric field can drive current. In turn, the induced current generates a magnetic perturbation (see Eq. (10.4)) and for field variations in the direction radial from Jupiter, the induced dipole would have the form inferred from Galileo measurements.

A test was designed to support the speculation that the observed magnetic perturbation was the signature of induction. A planned future flyby was modified so that closest approach to Europa would occur at a rotation phase of Jupiter for which the external radial field component would be in the direction opposite to that of the first pass. The orientation of a permanent internal magnetic moment would not change from one pass to another but, if the dipole were generated by induction, the internal magnetic moment would reverse between the two passes. The internal moment was found to reverse, thereby demonstrating that the observed dipole field was induced.

The next problem was to identify the layer in which the induced current flowed. Gravity measurements supplemented by knowledge of average composition have been used to model Europa's interior as a dense metallic sphere with radius between 0.3 and 0.5 R_E (R_E is the radius of Europa) surrounded by a rocky shell and covered by an ice shell of roughly 100 km depth. The magnetic perturbations recorded on Galileo's first flyby of Europa were just what would be observed if the varying field of Jupiter's magnetosphere was inducing current in Europa's interior. The near-surface signature of currents flowing in Europa's conducting core, whose radius is 0.5 R_E or less, would be at most $0.5^3 = 0.12$ smaller than observed because of the rapid fall-off with distance of the amplitude of a dipole field. In order to account for the size of the induced dipole moment, the induced current must have been flowing very near the surface of the moon. The outermost layer of Europa was known to be composed of light material, mainly H_2O, with an icy surface. Ice is a poor conductor of electricity. However, liquid water containing dissolved electrolytes, something like Earth's ocean, is a reasonably good electrical conductor that could easily carry the required current density. Thus, it seems extremely probable that the conducting layer near the surface is a global-scale ocean buried beneath the icy surface, an ocean discovered through magnetic field measurements and logical deductions from those measurements. Missions are being planned to continue the investigation of this intriguing feature of Europa.

10.6 Moons without atmospheres

Generic properties of the flow onto a non-conducting body were discussed above and some features are illustrated in Fig. 10.2a. The sketch, although simplified, represents the most important features of the interaction of the solar wind with the Moon and of Saturn's magnetospheric plasma with Rhea. Because there are no current paths through the moon, there is no compressional wave propagating upstream, so to a good approximation, the upstream plasma flows directly onto the surface, whether the moon is in the super-magnetosonic solar wind or in the sub-magnetosonic plasma of a planetary magnetosphere. The theoretical arguments have been thoroughly tested by analysis of data acquired by the Artemis dual spacecraft mission to the Moon using data from time intervals when one spacecraft was in the undisturbed solar wind and the other was in the near vicinity of the Moon (Zhang *et al.*, 2014). Even small changes in plasma properties can be identified in this manner. As seen in Fig. 10.7, just downstream of the Moon, the wake is devoid of plasma and $|\mathbf{B}|$ is larger than in solar wind. Plasma refilling is largely governed by MHD slow-mode speed, which is very slow, so the wake is still depleted of plasma at distances of 10 lunar radii downstream. The disturbance in the downstream region propagates away from the wake center at the fast-mode speed. As

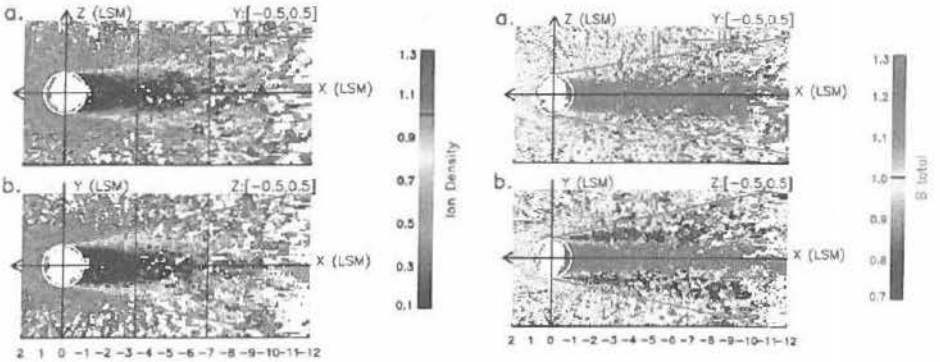

Fig. 10.7 Ion density (left) and magnetic field (right) in the vicinity of Earth's Moon from measurements by the *Artemis* spacecraft. The parameters represented by color are normalized by their values in the upstream solar wind. The x-axis is antiparallel to the solar wind flow. The data are plotted in the $x-z$ plane which is the plane of the solar wind field and the flow, and in the $x-y$ plane, perpendicular to this plane. The red lines diverging in the direction of negative x denote the wake boundary across which the density changes significantly. The divergence from the wake center is controlled by the propagation of fast mode waves. (From Zhang *et al.*, 2014.) A black and white version of this figure will appear in some formats. For the color version, please refer to the plate section.

anticipated for a non-conducting moon, no changes in plasma or field are evident upstream.

10.7 Moons with atmospheres or other sources of neutrals

The interaction between a moon and a flowing plasma differs greatly from the interaction described in Sect. 10.6 if a moon is enveloped in an atmosphere or another significant source of neutral gas. The upper levels of an atmosphere typically become ionized and capable of carrying current and we have already described how pickup ions and collisions with neutrals link allow currents to flow across the background field. Ionization of neutral gas scavenged from the upper atmosphere of the volcanic moon, Io, injects of order a ton of plasma per second into Jupiter's magnetosphere. Ionization of neutral gas from geyser-like plumes erupting from the surface of Enceladus injects tens of kilograms per second of plasma into Saturn's magnetosphere. Europa (at Jupiter) is an example of a moon with less intense sources of pickup ions, although there is some evidence for plumes arising from its surface. In all of these cases, the neutrals are central to the closure across the field of the Alfvén wing field-aligned currents that couple the moon with its parent planet.

Titan, Saturn's majestic moon that orbits at 20 R_S (Saturn's radius is 60 268 km) is shrouded in a very dense atmosphere. Its interaction region is exceptionally

complex because as it moves around Saturn the field and plasma conditions change significantly. Sometimes Titan even leaves the magnetosphere and finds itself embedded in the solar wind. At Titan, the interaction with the atmosphere produces strong draping of the field, creating a highly localized region of intense interaction.

We know little about Neptune's large moon, Triton, but there is evidence suggesting that, like Enceladus, it may have geysers jetting vapor from its surface and these may also modify its magnetospheric surroundings.

10.8 Small bodies in the solar wind

The discussions of interaction in the previous sections have assumed that the scale of the obstacle to the plasma flow is large compared with the gyroradius of a solar-wind ion so that analysis of the interaction in the MHD limit is appropriate. However, some bodies are so small that MHD no longer applies, and the form of the plasma interaction changes.

10.8.1 Asteroids

Asteroids are widely distributed in the inner solar system although their orbits cluster between the orbits of Mars and Jupiter. They range in size from ~1 km to ~500 km, too small to be plausible sources of dynamo magnetic fields. Little is known about their interaction with the solar wind. Much of what we know about asteroids is based on studies of meteorites, small bits of asteroidal matter that reach Earth from outer space and may be found on its surface. We know that many meteorites contain iron and are magnetized. This magnetization, referred to as remanent magnetization, suggests that the parent body of the meteorite may have had an internal dynamo that impressed a field on surrounding iron-bearing matter prior to the collision that broke it to pieces.

Little is known about the magnetic fields of asteroids. The Galileo spacecraft flew by two asteroids: Gaspra (scale length of order 14 km) and Ida (scale length of order 30 km). In both cases, small-scale but distinctive magnetic fluctuations lasting 5–10 min near closest approach were present in the measured magnetic field. It is plausible that the fluctuations were, in both flybys, linked to the nearby asteroid. However, one must recognize that fluctuations in the solar wind take many forms and it is possible that the signatures attributed to these bodies were fortuitous solar-wind fluctuations. Assuming that the signatures were generated by a plasma–asteroid interaction, the signatures were analyzed using an approach that applies for cases in which length scales are small compared with the ion gyroradius but large compared with the electron gyroradius. In this parameter regime, no shock is expected to form upstream because the relevant waves propagate faster than MHD

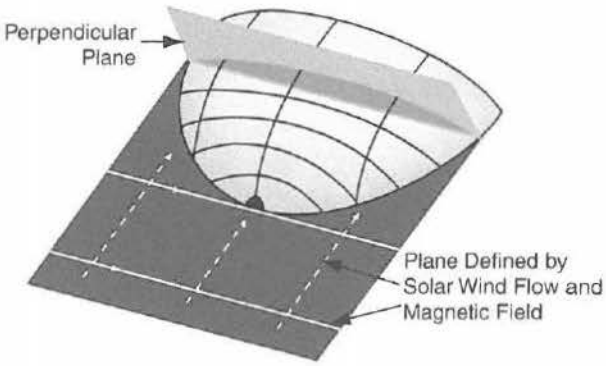

Fig. 10.8 Schematic of interaction region surrounding an asteroid of scale not large compared with ion gyroradii in the solar wind. Notice that the interaction region is extended along the field direction and compressed in the direction perpendicular to the field and the flow. (From Kivelson and Bagenal, 2007; credit: Steve Bartlett.)

waves. The interaction region is less cylindrical than that of a planet in the solar wind; it is compressed in the direction perpendicular to the field and the upstream flow as seen in the schematic illustration of Fig. 10.8. The duration of the signature associated with Gaspra required the asteroid to have a significant internal magnetic field corresponding to magnetization similar to that observed in some meteorites. This interpretation requires the parent body of Gaspra to have been magnetized before it broke up in some celestial collision. The Ida signature, also lacking an upstream shock, required that the body be conducting.

Magnetic-field perturbations near asteroid Braille are consistent with a specific moment (A m^2/kg) of the same order of magnitude as that inferred for Gaspra. By contrast, measurements taken by the NEAR-Shoemaker mission close to and on the surface of asteroid Eros indicate that its field is negligibly small, possibly because it is formed of magnetized rocks of random orientation. The DAWN spacecraft has spent months in the vicinity of asteroid Vesta and is off to an encounter with the largest asteroid, Ceres, but the spacecraft instrumentation does not include a magnetometer, so we have little information on the plasma interaction at these bodies. Other missions under discussion would add to our knowledge of asteroid magnetic properties.

10.8.2 Comets

Comets are small icy bodies that form in the outer solar system. The most spectacular ones are on highly elliptical orbits (on which they are likely to return to the inner solar system periodically) or sometimes on hyperbolic orbits (on which, in

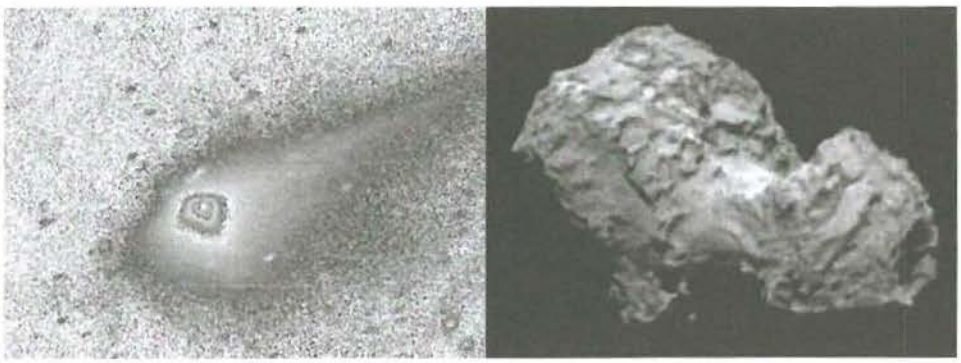

Fig. 10.9 Left: image of comet Churyumov–Gerasimenko from the 3.6 m telescope of the European Southern Observatory, La Silla/Chile. The comet was at 2.49 AU from the Sun when imaged on March 9, 2004. East is to the left and north is up. The nucleus is a source of asymmetric emissions. The scale is 70 000 km EW and 50 000 km NS. (From Glassmeier *et al.*, 2007.) Right: image of the nucleus acquired by Rosetta spacecraft on August 3, 2014. (Courtesy ESA/NASA – Rosetta spacecraft.)

the absence of significant perturbations, they are likely to escape the solar system). As these icy bodies approach the inner solar system, they are heated by the Sun and release neutral gas and dust, normally at rates that increase with approach to the Sun. The dust moves outward from the comet and, because it must conserve angular momentum, falls behind the comet increasingly as it moves farther outward, producing a tail that bends away from the direction radially outward from the Sun. The neutral gas can be ionized by solar ultraviolet radiation and the newly formed ions are picked up by the solar wind, as described in Sect. 10.5, forming a second tail directed radially outward.

Our understanding of cometary interactions will be greatly advanced by data acquired by the Rosetta spacecraft, which made measurements close to comet Churyumov–Gerasimenko, a 2-km object that reached perihelion in August of 2015. The image on the left of Fig. 10.9 shows the neutral and plasma environment, with a tail that extends tens of thousands of kilometers even though the comet is still far outside of Earth's orbit (2.49 AU). The tail is likely to extend over AU as the comet comes closer to the Sun. Comet Churyumov–Gerasimenko is a highly irregular object, heavily scarred by impacts as seen in an image taken as the spacecraft closed in on its target (Fig. 10.9 right). Often comets are described as dirty snowballs, but this comet, though dirty, is far from a ball-shaped object.

The solar wind flow is super-magnetosonic relative to the comet, but the flow slows as the wind approaches the comet because of its interaction with

the cometary material. As its momentum decreases, the Mach number of the interaction also decreases. Because of the decreasing Mach number, shocks upstream of comets may be quite weak or possibly even disappear. As the slowed flow carries magnetic flux past the comet, the solar-wind magnetic field gets hung up on the region near the comet and the field drapes around the slowed region in the form of a hairpin. The oppositely directed draped fields on the downstream side of the comet can reconnect, and cause a portion of the ion tail to break off. For reviews of interaction of the solar wind with Comet 67P see Hansen *et al.* (2007) and Rubin *et al.* (2014).

10.8.3 Pluto

The New Horizons spacecraft is en route to Pluto, the most accessible dwarf planet. At this time, only computer simulations can hint at what kind of interaction will be observed. The spacecraft lacks a magnetometer, so there will be no direct measurement of the planetary magnetic field, but plasma measurements should reveal whether there is an upstream shock and the nature of the flow in the vicinity of Pluto (McNutt Jr. *et al.*, 2008; McComas *et al.*, 2008). The parameters of the plasma interaction anticipated lead us to expect a very asymmetric magnetosphere because the gyroradii of solar wind ions are not small compared with Pluto's radius, implying that an MHD analysis will not apply (e.g., Delamere, 2009). Pluto's orbit is very eccentric. Only near perihelion, when its orbit lies closest to the Sun, does Pluto have an atmosphere. The magnetosphere is affected by an atmosphere, so there may be different forms of the interaction at different orbital phases (Bagenal *et al.*, 1997).

10.9 Summary and expectations for other planetary systems

Plasma flowing onto the small bodies of the solar system creates interaction regions of many sorts, some very localized and others extended over many AU. Interpreting the response has required us to consider the scale of the body relative to fundamental length scales of the incident plasma, to note whether or not the body conducts electrical current, and to consider the neutral gas environment of the body. Dimensionless parameters of the incident plasma and the size of the body relative to the ion gyroradii of the incident plasma were found to be critical in determining the global structure of the interaction region and whether or not it was bounded by a shock on the upstream side.

Based on what we know from studies of bodies in the solar system, one can speculate on the nature of the interaction in systems that have not yet been explored.

Further from the Sun than the orbit of Neptune lie dwarf planets similar to Pluto but located in even more tenuous solar wind. The different plasma environment may modify the response in interesting ways.

Planets around stars other than the Sun are being discovered continually (see Ch. 6 for a discussion of exoplanet dynamos, and Ch. 5 of exoplanet discoveries). The conditions relevant to the formation of a magnetosphere may differ immensely if stellar winds differ substantially from the solar wind. One can be reasonably certain that there will be surprises whenever our measurements of other stellar systems begin to provide measurements of extrasolar magnetospheres.